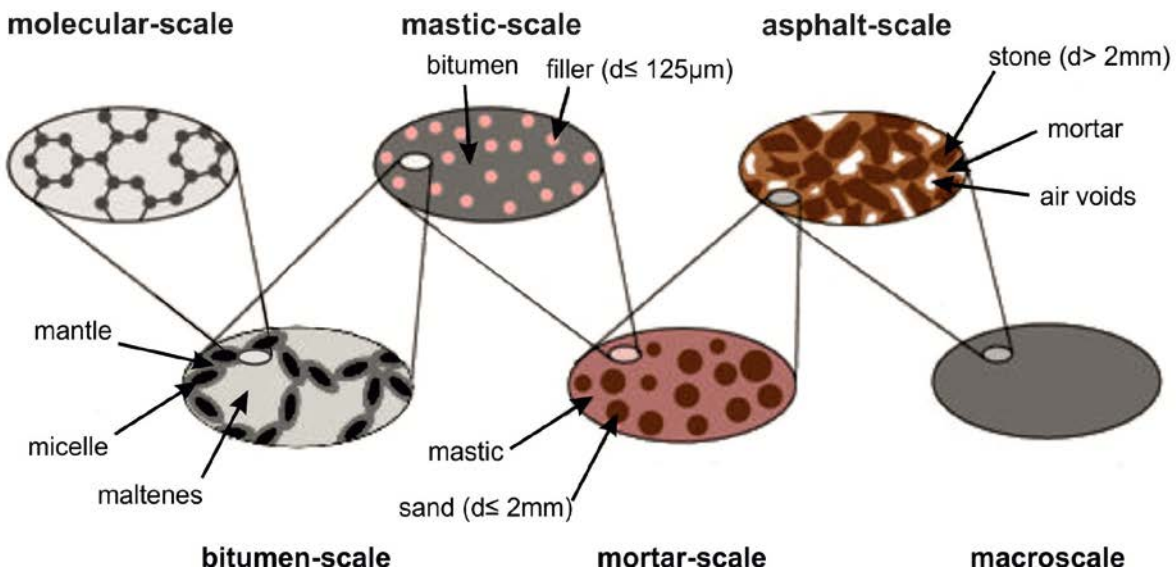


1 Bitumen is broadly defined as a *virtually not volatile, adhesive and waterproofing material*
 2 *derived from crude petroleum, or present in natural asphalt, which is completely or nearly*
 3 *completely soluble in toluene, and very viscous or nearly solid at ambient temperatures* [1]. This
 4 definition is as exact as possible, given the diversity of bitumina.

5 Since materials researchers started investigating bitumen several models for the bitumen
 6 microstructure and asphalt concrete were developed. This study is based on the micelle theory
 7 [2], [3] and the extended 5+1 scales of asphalt observation model [4], which points out the
 8 importance of the molecular and bitumen scale analysis for the material properties (**FIGURE 1**).
 9 Basically, this model assumes bitumen to be a colloidal system of asphaltenes micelles dispersed
 10 in a maltene matrix.



12 **FIGURE 1: The 5+1 scales of asphalt observation, explaining the relations of material**
 13 **properties to the different scales of study** [4]
 14

15
 16 CLSM is an imaging technique capable of analyzing highly localized fluorescence
 17 emission and was used to visualize the bitumen microstructure. Additionally, fluorescence
 18 spectroscopy was employed to obtain integrated spectra of bitumen and bitumen fractions. By
 19 combining the information, we were able to develop a new model hypothesis for bitumen ageing.

20 Previous studies employing CLSM on bitumen have mainly been focused on SBS-
 21 modified bitumina [3], [5], [6], [7], [8]. The analysis of pure bitumen with this intriguing method
 22 was seldom conducted [9], [10], [8]. The discussion of the nature of the fluorescent centers that
 23 can be visualized by CLSM is an ongoing debate in bitumen research [11]. Contradictory
 24 identifications range from asphaltenes [10], [9] to waxes [12]. Some of these hypotheses can be
 25 discarded easily, since certain constituents are not capable of fluorescent emission in the visible
 26 range due to their very physical and chemical nature. This study has identified the origin of these
 27 fluorescent centers and found conclusive evidence that the aromatics fraction is the source of the
 28 strong fluorescent signals in bitumen that can be visualized by CLSM.
 29

1 **2. MATERIALS AND METHODS**

2 **BITUMEN AND BITUMINOUS SPECIMEN**

3
4
5
6
7
8
9

The materials used in this study were carefully chosen for their material properties and their respective position in the production cycle of bitumen (**TABLE 1**). The precursors were studied to examine, if they exhibit a similar structural composition to their respective end products. Bitumen B50/70 was chosen as a typical material used in road construction, while B70/100 bitumina are often used for the production of SBS-modified bitumina.

10

TABLE 1: Samples and Description

Sample	Description
Precursor 1	Vacuum flashed, cracked residuum
Precursor 2	Residuum of vacuum distillation
B50/70	Bitumen for asphalt concrete production
B70/100 1	Bitumen for asphalt concrete production or for production of SBS-modified Bitumina
B70/100 2	Bitumen for asphalt concrete production or for production of SBS-modified Bitumina

11

12 **ANALYTICAL EQUIPMENT**

13

14 We employed an ECLIPSE TE2000 (Nikon Corporation, Tokyo, Japan) as a confocal
15 laser scanning microscope. The microscope hosts both a transmission and a CLSM (Confocal
16 Laser Scanning Microscope) array. The light source for the transmission array is a T-DH 100W
17 Illumination Pillar (Koehler Type). An Argon-ion laser is used as source of excitation radiation.
18 Typical for CLSM, laser optics is configured to allow a scanning of the surface and the image is
19 created point by point and line by line. The advantages mentioned above in combination with the
20 highly sensitive detector are key features for the successful application. However, the capability
21 to scan volumes below the surface, a key advantage of the CLSM technique, cannot be applied
22 here, because of the high absorption cross section in the visible range of all bitumina. For sample
23 preparation, the bitumen was heated to about 150-200°C as necessary for melting the sample.
24 Then a small quantity of bitumen was applied to a glass slide with a piece of wire and a second
25 glass slide was placed onto the sample. After a short period of cooling, the sample was
26 measured. Early experiments showed that this procedure had to be modified. The first step
27 towards a significant improvement in picture quality is the replacement of the standard object
28 carriers by extremely thin glass slides (<0,5mm). Second, an additional heating period was
29 implemented, allowing the bitumen film to spread and become thinner. These very thin films
30 could then be examined by CLSM.

31

32 For fluorescence spectroscopy, an Edinburgh Instruments FSP920 photoluminescence
33 spectroscopy setup was at our disposal. As an illumination source, a XE900 Xenon Arc Lamp is
34 used, which provides high intensity radiation on a broad spectrum. The setup employs double
35 Czerny-Turner monochromators (type TMS300) at both excitation and emission arms,
36 guaranteeing a very narrow spectral bandwidth. The detector is a S900 single-photon
37 photomultiplier (type R928). The spectrometer was used to conduct both excitation and emission
measurements. For sample preparation, the bitumina were heated to 150°C and a drop of

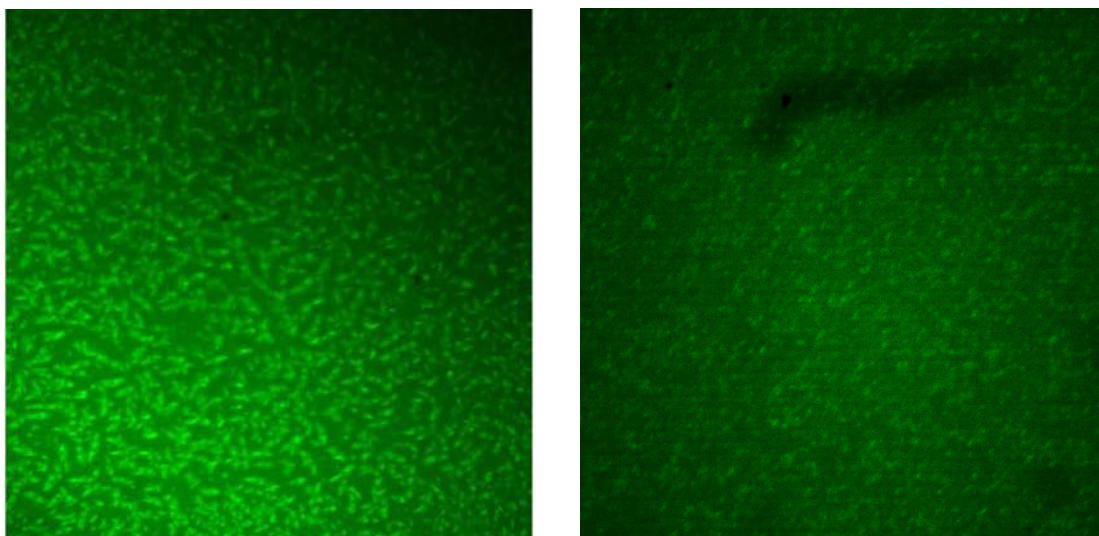
1 bitumen was applied to a standard microscopic slide. This slide was stored at the same
2 temperature for 5 minutes to allow the drop to spread and increase its surface. Afterwards the
3 samples were cooled to room temperature and subjected to fluorescence spectroscopy. For
4 bitumen fractions, this treatment was not necessary, because the maltene phase and its
5 components are viscous liquids at room temperature and can be applied directly to the glass
6 slide. The asphaltenes were taken up with toluene and then dripped slowly on the warm glass
7 surface (80°C) to allow the formation of a thin film.

8 Chromatographic separation was conducted according to ASTM Standard 4124 [13],
9 which is the most prominent and widely used method [11] and based on the Corbett procedure
10 [14]. However, the nomenclature was changed to fit the SARA (Saturates Aromatics Resins
11 Asphaltenes) scheme, deviating from the standards nomenclature (aromatics – naphthene
12 aromatics; resins – polar aromatics). First bitumen was separated into maltene and asphaltene
13 phase by extraction with n-heptane. However, the n-heptane extraction was conducted in a
14 Soxhlet-extractor. The further separation is conducted in a 1000mm chromatographic column
15 with alumina as the stationary phase with three different solvents/solvent combinations. The
16 eluate was collected in 50ml beakers, which were sealed, cooled, and then stored at -15°C to
17 slow oxidative degradation. Then each fraction was warmed to room temperature and subjected
18 to distillative separation under vacuum. The sample was then cooled to room temperature before
19 breaking the vacuum. Afterwards, the fraction was weighed. The sample was then again
20 subjected to escalating distillation (max 185°C, 10mbar, 10min) and weighing until constant
21 weight was reached to assure gravimetric exact measurements. Then the sample specimens were
22 prepared for fluorescence spectroscopy.
23

24 **3. RESULTS**

25 **3.1 Microstructure of Bitumen, Bitumen Precursors**

26
27 It was possible to obtain new and enhanced pictures of the bitumen microstructure by
28 application of CLSM to pure bitumina. These images proof the existence of a microstructure,
29 which implicates agglomeration processes and phase separation processes in bitumen, as
30 implicated in the micelle model. The fluorescent centers detected are of roughly ellipsoid shape,
31 vary in size and amount, and their spatial distribution seems to be statistical and unordered.
32 Exemplary, two images are shown in FIGURE 2. Their exact size distribution and population
33 density varies for each sample and is characteristic for specific bitumina. The micelle model
34 describes bitumen as a colloidal system of dispersed asphaltenes in a continuous maltene phase,
35 which makes the spatial distribution of the fluorescent centers an important issue [3], [11]. Thus,
36 a strong connection to the mechanical and rheological properties can be assumed. Preliminary
37 experiments with picture analysis software have been conducted to assess the particle size
38 distribution for the tested bitumina and whether significant differences between the samples can
39 be found. Although the necessary picture processing is a rather complicated task due to high
40 background fluorescence in bitumen, first results are promising and future experiments and
41 process automation could provide a powerful tool for bitumen analysis.
42

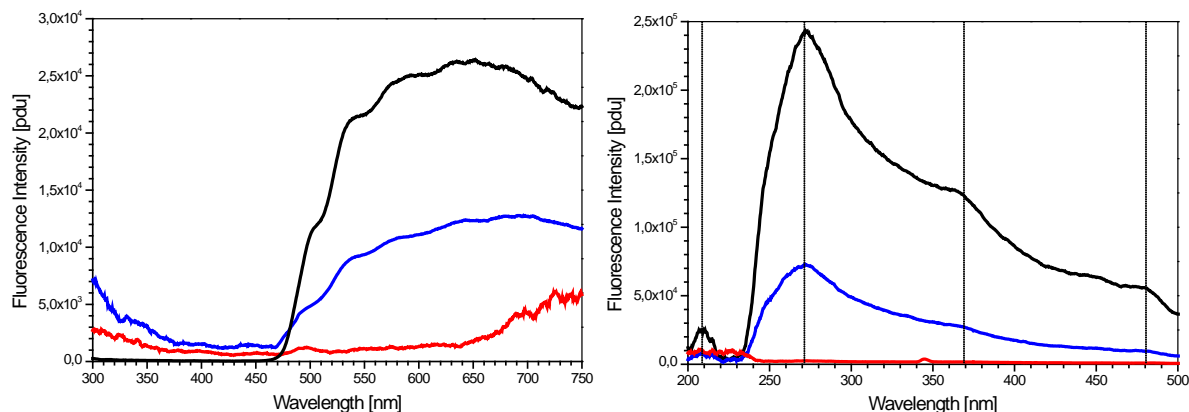


1
2 **FIGURE 2: CLSM images of bitumen precursor PE1005 (left) and bitumen B70/100**
3 **(right), fluorescent centers characteristic for the respective sample**

4
5 **3.2 Fluorescence Analysis and Chromatographic Separation**

6
7 Initially, fluorescence experiments have been conducted to support the use of CLSM as
8 an imaging technique on bitumen. However, this study found that besides the distribution of
9 fluorescent centers, the fluorescent behavior of bitumen and bitumen fractions can provide
10 additional evidence regarding the actual microstructure of bitumen. Fluorescence spectroscopy
11 yields an integrated spectrum that is not capable of visualizing spatial distributions. Information
12 about the fluorescent centers and their composition in bitumen must be obtained indirectly
13 through inference. A closer look on the basic physicochemical properties of bitumen reveals that
14 bitumen contains only three fractions that could theoretically be the origin of the fluorescent
15 signal. The asphaltenes, the resins, and the aromatics are, based on their general description,
16 capable of fluorescence. Saturates can easily be dismissed as a source of fluorescent emission,
17 due to the well defined chemical nature of fraction. There are two kinds of spectra presented
18 here, excitation scans (variable excitation, fixed detection wavelength) and emission scans (fixed
19 excitation, variable detection wavelength). For the excitation scans, the same detection
20 wavelength as used at the microscope was chosen, 515nm, and a spectral range of 200-500nm
21 was observed. For the emission spectra, two wavelengths have been studied carefully. First the
22 excitation wavelength of 488nm was selected, because this is one of the excitation wavelengths
23 available in the CLSM setup. To check for high energy fluorescence transitions, we employed a
24 wavelength of 280nm. (FIGURE 3).

25
26
27
28
29



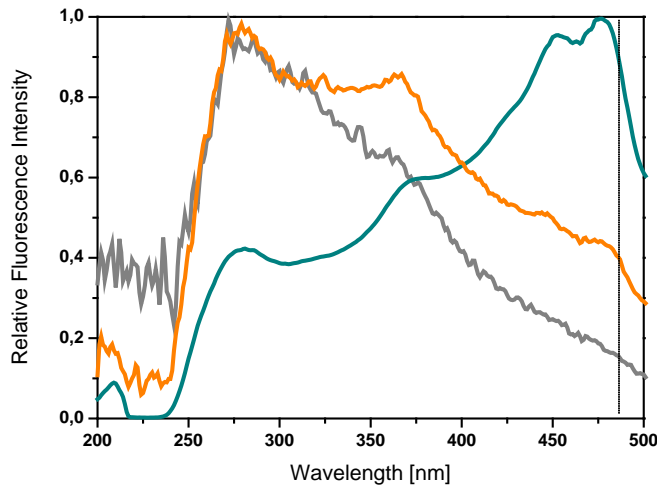
1
2
3 **FIGURE 3: Emission fluorescence spectra of bitumen B50/70 (blue), asphaltenes (red)**
4 **and maltenes (black) at 280nm excitation wavelength (left) and excitation spectrum of**
5 **bitumen B50/70 at 515nm detection wavelengths;**

6 The excitation fluorescence spectrum of pure bitumen allows the identification of four
7 wavelength of particular interest (**FIGURE 3**, right): 210nm, 270nm, 370nm, 480nm (dotted
8 lines) for CLSM at a detection wavelength of 515nm. These are a local and the absolute
9 maximum, as well as the two shoulders visible in the excitation scan of the pure bitumen. The
10 distribution of the fluorescent centers excited at these wavelengths would be of particular
11 interest. Since fluorescence transitions can also be triggered by wavelengths lower than the
12 necessary minimum, it is impossible to visualize the higher energetic transitions exclusively. For
13 the CLSM studies, an excitation wavelength of 488nm was chosen, because it is very close to the
14 shoulder at 480-490nm. Also it is one of the spectral lines providing the highest intensity
15 available at the Argon-ion laser and is frequently used for CLSM. The technique was capable of
16 revealing the origin of the fluorescence signals of the different species spatially distributed.

17 After the completion of the CLSM imaging, soon investigating the source of the
18 fluorescence became a primary goal of further experiments. Usually a detailed interpretation of
19 the fluorescence spectra could be attempted, but for bitumen, this is a rather difficult task. The
20 dependency of fluorescence phenomena on the chemical vicinity of the molecules is very well
21 documented and the effects of the surroundings are hardly assessable for bitumen [15]. Hence, a
22 more empirical approach was chosen. The fractionation by chromatography is a well-known and
23 reliable standard method in bitumen analysis [14], [13], [11]. It is often employed for
24 characterization of bitumina by their relative contents of fractions. The fractions themselves
25 again are complex mixtures of molecules, but exhibit similar chemical/physical behavior. In
26 previous publications, the origin of fluorescence emission was suspected to be the asphaltenes
27 fraction. This theory was explored to full extent. In general asphaltenes are defined as insoluble
28 in n-heptane. While the basic extraction protocol for standardized testing is based on a simple
29 extraction with n-heptane [13], for these experiments, a Soxhlet-extractor was used for the
30 removal of asphaltenes, which guarantees as pure asphaltenes as reasonably possible. The
31 fluorescence spectra of these fractions were surprising. Our experiments strongly indicated that
32 the origin of the fluorescent centers can be found in the maltene phase and not in the asphaltenes
33 phase, as proposed by other researchers [10]. The spectra of the asphaltenes show almost no
34 fluorescent capabilities at either the detection wavelength or the excitation wavelength used by
35 the CLSM (**FIGURE 3**). The maltene phase exhibits strong fluorescence in these areas. The

1 absolute intensity ratings, although being only general tendencies, suggest that the residuum
2 somehow dampens the fluorescence of the pure bitumen 50/70 as it dilutes the extract.
3 Obviously, the fluorescence of the asphaltenes is shifted to wavelengths higher than 750nm, into
4 the near infrared region, which is not accessible to the fluorescence spectroscopy used in this
5 study.

6 Further fractioning of the maltene phase into saturates, aromatics, and resins, was
7 conducted to obtain their respective spectra. Although the spectra differ within reasonable
8 bounds, all bitumina show the same behavior: Only the aromatics fraction shows significant
9 fluorescence in the relevant areas. Taking into account the micelle model and that the fluorescent
10 centers are spatially distributed and the fluorescent species seem to agglomerate, they can be
11 interpreted as a stabilizing mantle, composed mainly of aromatics, surrounding the asphaltenes
12 micelles. FIGURE 4 shows the normalized spectra of the bitumen fractions and show that the
13 aromatics exhibit very strong fluorescence at 480nm excitation. However, it has to be added that
14 normalization removes the information of fluorescent emission intensity, which is by several
15 orders of magnitude higher for the aromatics than for both resins and saturates.
16

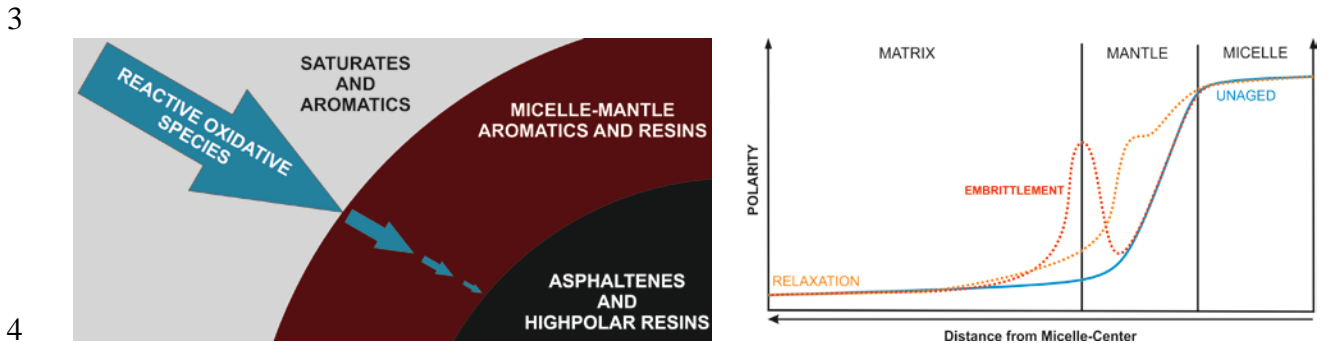


17
18 **FIGURE 4: Fluorescence spectra of bitumen fractions: saturates (grey), aromatics**
19 **(green), resins (yellow), detection wavelength of CLSM: 488nm**

20
21 **3.3 The Micelle Model and Ageing**

22 Considering this new information about the chemical structure of the micelle we
23 formulated a new thesis regarding bitumen ageing. This model is a refinement of the micelle
24 model and takes the research conducted upon the oxidative properties of bitumen and bitumen
25 fractions [16], [11] into special consideration. The saturated fraction is considered the least
26 reactive, almost inert by comparison, of all fractions. The asphaltenes seem to have a very strong
27 capability for oxidation in liquid state (i.e. melted or in solution), but show low reactivity at
28 ambient conditions due to their highly associated and solid state. Both aromatics and resins show
29 significant susceptibility for oxygen uptake [16]. Due to this research, for mixing and
30 construction, i.e. the first short term ageing step, oxidation can take place across all phases, with
31 the exception of saturates, but for long term ageing, the oxidation of the asphaltenes fraction has
32 to be considered insignificant. Based on the micelle structure model and its structural and

1 chemical constraints, a pathway for oxidative species diffusing through the material can be
2 plotted (FIGURE 5, left).



4
5 **FIGURE 5: Reactive oxidative species (ROS) pathway in bitumen (left). Polarity of**
6 **bitumen in the micelle structure in fresh (blue), long term aged (red), and relaxed (orange)**
7 **state (right)**

8
9 The continuous phase is largely inert, so the first contact between oxidative species and reactive
10 material happens at the surface of the micelle mantle, which is composed of aromatics and
11 resins. There oxidation can occur and the amount of reactive oxidative species reaching the
12 asphaltenes has to be considered reduced strongly by the oxidation happening in the mantle. This is
13 also conclusive with studies on asphalt oxidation which generally show a declining amount of
14 nonpolar aromatics and a buildup of resins and asphaltenes as a result of ageing. This oxidation
15 process has to be considered very slow in nature, due to the low temperature and the stability of
16 most carbohydrates to oxidation at ambient conditions. However, experience in road engineering
17 show that road damages due to asphalt ageing can occur few months after the construction.
18 Furthermore, experiments regarding asphalt healing in lying asphalt concrete roads show that
19 heating the asphalt can significantly increase road lifetime by enabling self healing [17]. Based
20 on this research we developed a new model hypothesis for asphalt ageing. If the low mobility of
21 molecules at ambient conditions is taken into account, it can be understood that oxidation leads
22 to the formation of a high polar layer on the outside of the micelle mantle. If the polarity reaches
23 a certain limit, then phase separation at this new boundary occurs and the whole, larger micelle
24 plus mantle particle basically forms another immobile center. This reduces transduction of elastic
25 properties and leads to a hardening of the material. If the asphalt is heated, then the diffusion rate
26 significantly increases and the now highly polar resins/aromatics migrate into the center of the
27 micelle and the functionality of the mantle is restored. This also explains why the ageing at road
28 construction is not as destructive as it would have to be considered. At the high temperatures, the
29 high polar oxidation products can simply be transported into the inside of the micelle. However,
30 the increase in micelle volume means that the mantle becomes thinner and thus the polarity
31 gradient more extreme and micelle mobility in the matrix decreases. This limits the capability of
32 relaxation by inclusion of high polar molecules in the micelles.

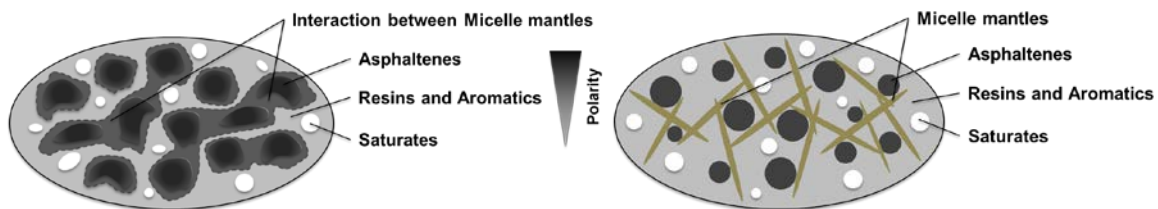
33

34 **4. MICROMECHANICAL MODELING OF BITUMEN MICROSTRUCTURE**

35 Based on the micelle model introduced before, delivering a basic concept of the bitumen
36 microstructure, and the knowledge gain through the proposed results of chemical analysis, a
37 mechanical model which takes the bitumen microstructure into account could be derived.

1 Therefore, the framework of continuum micromechanics was chosen, allowing for a description of
2 the viscoelastic response of bitumen depending on the volumetric composition and the physical
3 properties of its constituents. Moreover, the interaction between material phases can be taken
4 into account through different so-called homogenization schemes [18], [19], [20], [21], [22],
5 [23]. Thereby, a material is considered as a micro-heterogeneous body filling a macro-
6 homogeneous representative volume element (RVE). Quasi-homogeneous subdomains [20], [21],
7 [22], also known as material phases, with known physical properties describe the microstructure
8 within such an RVE. Correlating the homogeneous deformations acting on the boundary of an
9 RVE with the resulting (average) stress, the mechanical behavior of the overall material can be
10 estimated. Such an approach is referred to as homogenization.

11 On the basis of the chromatographic separation mentioned before, a reasonable
12 subdivision of bitumen into distinct material phases for the micromechanical modelling were
13 possible (see **FIGURE 6**). Therefore, an RVE of bitumen is built up by a contiguous matrix
14 phase, representing aromatics and resins, in which spherical inclusions are embedded, describing
15 the saturates. While the asphaltenes, acting in the center of micelles, are also modelled by
16 spherical inclusions, the micelle mantles are assumed to form a network-like structure and for
17 this reason are represented by needles with randomly distributed orientations.
18



19

20

21

FIGURE 6: Concept of bitumen microstructure based on micelle model and therefrom derived RVE considered in micromechanical model

22

23 Identification of the viscoelastic behavior of the maltene phase (matrix phase and the inclusions
24 representing the saturates) was done by static shear creep tests using a dynamic shear rheometer
25 (DSR). As asphaltenes and their mantle material (highly polar resins and aromatics) act together
26 in the micelle structure, the same effective viscoelastic behavior is assigned to both phases. To
27 access this effective behavior, static shear creep tests on bituminous mixtures with different
28 (known) asphaltene contents were carried out and by comparison of experimental and model
29 results on a best-fit basis the material behavior could be obtained. In addition, the increase of
30 needles, representing the interaction between micelles, with increasing asphaltene content could
31 be determined, revealing an exponential relationship for asphaltene contents between 0 % and
32 20 %. For a detailed validation of these assumptions and the introduced micromechanical model
33 we refer to further publications.

34

35

36

37

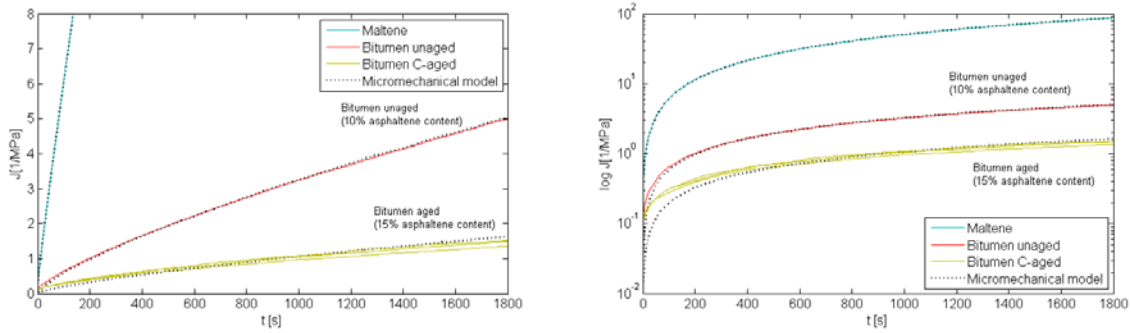
38

39

40

41

The influence of long-term ageing was investigated on B70/100 bitumen samples, aged in
laboratory using PAV and RTFOT equipment [24]. From static shear creep tests on these
samples it was found, that the mechanical behavior of asphaltenes as well as maltenes due to
ageing is negligible. However, a significant increase in asphaltene content, and consequently the
micelle mantle content, could be observed (detailed information also presented in further
publication). This increase, and thus the effect of ageing, can be described satisfactorily by the
derived micromechanical model, as can be seen in **FIGURE 7**.



1
2 **FIGURE 7: Comparison of experimental results on aged and unaged bitumen (B70/100 at**
3 **+5°C) from static shear creep tests with predictions from micromechanical modeling**
4

5 **5. CONCLUSION**

6 Confocal laser scanning microscopy is an important tool for bitumen analysis, because of
7 its capability to visualize the microstructure of bitumen. It proves the existence of two separate
8 phases in bitumen, as predicted by the micelle theory. Also, it was possible to identify the
9 fluorescent phase in bitumen by chromatography and fluorescence spectroscopy as the aromatics
10 fraction. The aromatic phase contains the molecules that exhibit strong fluorescence capabilities
11 at 488nm excitation and 515nm detection and seem to agglomerate. Although other phases also
12 show activity under these conditions, it is by several orders of magnitude lower in intensity, if
13 compared to the aromatics. Thus, an ongoing debate in the scientific community has found its
14 end.

15 The realization that the fluorescent phase in bitumen is actually the aromatics phase
16 indicates that this is a critical phase regarding ageing and embrittlement. Basically, we developed
17 an enhanced micelle theory for ageing that is capable of explaining the different effects of short
18 term and long term ageing as well as thermal healing of asphalt concrete. This is an early step on
19 the road to upstream recycling of asphalt concrete and bitumen, because the identification of
20 problematic structural and chemical changes is necessary to overcome their effects.

21 Based on the introduced micelle model, a mechanical model is derived in the framework
22 of continuum micromechanics considering bitumen as a four-phase composite consisting of
23 asphaltenes, micelle mantles, and saturates embedded in a contiguous matrix of aromatics and
24 resins. The microstructure was implemented in a homogenization scheme to predict the overall
25 viscoelastic response. An increase of asphaltene content, and thus volume content of the micelles,
26 is identified to be responsible for ageing effects, which can be described by the micromechanical
27 model very well.
28
29

1 6. REFERENCES

- 2 [1] European Committee for Standardization. EN 12597: Bitumen and bituminous binders –
3 Terminology. Brussels: European Committee for Standardization, 2012.
- 4 [2] Sheu E.Y. Physics of asphaltene micelles and microemulsions—theory and experiment,
5 *Journal of Physics: Condensed Matter*, 8/1996, pp. A125-A141. 1996.
- 6 [3] Loeber L., Muller G., Morel J., Sutton O. Bitumen in colloid science: a chemical, structural
7 and rheological approach, *Fuel*, 77/13, pp. 1443-1450. 1998.
- 8 [4] Lackner R., Spiegl M., Blab R., Eberhardsteiner J. Is Low-Temperature Creep of Asphalt
9 Mastic Independent of Filler Shape and Mineralogy? – Arguments from Multiscale Analysis,
10 *Materials in Civil Engineering*, 17/5, 2005, pp. 485-491. 2005.
- 11 [5] Sengoz B., Isikyakar G. Analysis of styrene-butadiene-styrene polymer modified bitumen
12 using fluorescent microscopy and conventional test methods, *Journal of Hazardous Materials*,
13 150/2008, pp. 424-432. 2008.
- 14 [6] Topal A. Evaluation of the properties and microstructure of plastomeric polymer modified
15 bitumens, *Fuel Processing Technology*, 91/1, 2010, pp. 45-51. 2009.
- 16 [7] Fawcett, A.H., McNally, T. Polystyrene and asphaltene micelles within blends with a
17 bitumen of an SBS block copolymer and styrene and butadiene homopolymers, *Colloid and*
18 *Polymer Science* 281/3, 2003, pp. 203-213. 2003.
- 19 [8] Handle F., Grothe H., Neudl S. Confocal Laser Scanning Microscopy – Observation of the
20 Microstructure of Bitumen and Asphalt Concrete, 5th Eurasphalt & Eurobitume Congress,
21 Istanbul, Turkey, P5EE-188. 2012.
- 22 [9] Forbes A., Haverkamp R.G., Robertson T., Bryant J., Bearsley S. Studies of the
23 microstructure of polymer-modified bitumen emulsions using confocal laser scanning
24 microscopy, *Journal of Microscopy*, 204/3, 2001, pp. 252-257. 2001.
- 25 [10] Bearsley S., Forbes A., Haverkamp R. Direct observation of the asphaltene structure in
26 paving-grade bitumen using confocal laser-scanning microscopy, *Journal of Microscopy*, 215/2,
27 2004, pp. 149-155. 2004.
- 28 [11] Lesueur D. The colloidal structure of bitumen: Consequences on the rheology and on the
29 mechanisms of bitumen modification, *Advances in Colloid and Interface Science*, 145. pp. 42-
30 82. 2009.
- 31 [12] Lu X., Langton M., Olofsson P., Redelius P. Wax morphology in bitumen, *Journal of*
32 *Materials Science*, 40, 2005, pp. 1893-1900. 2005.
- 33 [13] American Society for Testing and Materials. ASTM D4124-01 - Standard Test Methods for
34 Separation of Asphalt into Four Fractions, ASTM International, 2010.
- 35 [14] Corbett LW. Composition of asphalt based on generic fractionation, using
36 solventdeasphalting, elution-adsorption chromatography and densimetric characterization.
37 *Analytical Chemistry*, 41, pp. 576–579. 1969.
- 38 [15] Tucker S., Jason M., Acree W., Zander M., Mitchell R. Spectroscopic Properties of
39 Polycyclic Aromatic Compounds Part IV: Effect of Solvent Polarity and Nitromethane on the
40 Fluorescence Emission Behaviour of Select Bipolycyclic Aromatic Hydrocarbons, *Applied*
41 *Spectroscopy*, 48 (4), pp. 458-464. 1994.
- 42 [16] Peterson J.C. A Review of the Fundamentals of Asphalt Oxidation – Chemical,
43 Physicochemical, Physical Property, and Durability Relationships. Transportation Research
44 Board, Washington, DC 20001, 2009.

- 1 [17] Qiu J., Molenaar A.A.A., van de Ven M.F.C., Wu S., Yu J. Investigation of self healing
2 behaviour of asphalt mixes using beam on elastic foundation setup, *Materials and Structures*, 45,
3 pp. 777-791. 2012.
- 4 [18] Hill R. Elastic properties of reinforced solids: some theoretical principles, *Journal of the*
5 *Mechanics and Physics of Solids*, 11, pp. 357-362. 1963.
- 6 [19] Hill R. Continuum micro-mechanics of elastoplastic polycrystals, *Journal of the Mechanics*
7 *and Physics of Solids*, 13(2), pp. 89-101. 1965.
- 8 [20] Suquet P. *Continuum micromechanics*, Edition 1997, Wien – New York, Springer, 1997.
- 9 [21] Zaoui A. Structural morphology and constitutive behavior of microheterogeneous materials.
10 in[20] Wien – New York, Springer. pp. 291-347. 1997.
- 11 [22] Zaoui A. Continuum micromechanics: survey. *Journal of Engineering Mechanics (ASCE)*,
12 128(8), pp. 808-816. 2002.
- 13 [23] Scheiner S., Hellmich C. Continuum microviscoelasticity model for aging basic creep of
14 early-age concrete. *Journal of Engineering Mechanics*, 135(4), pp. 307-323. 2009.
- 15 [24] Huang S. C., Tia M., and Ruth B. E. *Laboratory Aging Methods for Simulation of Field*
16 *Aging of Asphalts*, *Materials in Civil Engineering*, 1996.